DUV LITHOGRAPHY (KrF) FOR 130 nm USING OFF-AXIS ILLUMINATION AND ASSISTING FEATURES

Jo Finders, Jan van Schoot, Melchior Mulder, Adolph Hunter[a],
Mircea Dusa[b], Bob Socha[c], Peter Jenkins[d]

[a]ASML, De Run 1110, 5503 LA Veldhoven, The Netherlands
[b]ASML, 8555 S River Parkway,Tempe, AZ, USA
[c]ASML Masktools, 2833 Junction Avenue, Suite # 101, San Jose, CA, USA
[d]ASML, Suite 603, 6/F, One International Finance Center, 1 Harbour View Street, Central, Hong Kong, SAR

This paper was first presented at the
Semicon / Japan '99, SEMI Technology Symposium
December 1999, Makuhari Messe, Chiba, Japan

DUV LITHOGRAPHY (KrF) FOR 130 nm USING OFF-AXIS ILLUMINATION AND ASSISTING FEATURES

Jo Finders, Jan van Schoot, Melchior Mulder, Adolph Hunter[a],
Mircea Dusa[b], Bob Socha[c], Peter Jenkins[d]

[a]ASML, De Run 1110, 5503 LA Veldhoven, The Netherlands
[b]ASML, 8555 S River Parkway,Tempe, AZ, USA
[c]ASML Masktools, 2833 Junction Avenue, Suite # 101, San Jose, CA, USA
[d]ASML, Suite 603, 6/F, One International Finance Center, 1 Harbour View Street, Central, Hong Kong, SAR

ABSTRACT

To meet the industry's timing for 130 nm production, different optical lithography solutions are being considered. Due to the maturity of the resists and optical materials, the application of high NA (≤ 0.70) KrF excimer laser exposure tools, together with resolution enhancement techniques, is an attractive solution.

There are two main enhancement techniques to extend KrF lithography. The first utilizes alternating phase shift masks. This technique works for both dense lines and isolated lines. The second method involves the use of off-axis illumination such as annular and quadrupole. Off-axis illumination is a very effective enhancement technique for dense lines. However, it is not applicable to fully-isolated lines because of the inherent differences in diffraction pattern. Applying scattering bars (also called assisting features) to an isolated line modifies the diffraction pattern. This diffraction pattern is similar to that generated by dense lines. In this way off-axis illumination can be applied to enhance the depth of focus and exposure latitude of fully-isolated lines in the same manner as dense lines.

In this paper, we will show the lithographic performance of a high NA KrF Step & Scan system (PAS 5500/700) when used to image 130 nm lines. Results will be shown with both annular and QUASAR™ off-axis illumination techniques applied to enhance the process windows of both dense lines, and isolated lines with scattering bars.

1. BACKGROUND

Advances in optical lithography have been critical to the dramatic growth of the IC industry through enabling continuous improvement in the cost per function. This has been achieved by enabling economic implementation of smaller design rules and larger die sizes. Moore's Law, which predicts that there is a doubling in circuit complexity every year, describes this observed exponential improvement [1]. This was historically achieved through a combination of a reduction in design rules, an increase in die sizes and advances in process architecture and circuit design. Since the mid-1990s the rate of design rule evolution has moved from a 3-year to a 2-year cycle. This equates to a change from 10% per year to 15% per year in the reduction of the minimum feature size implemented in leading edge production (see Figure 1, Lithography Roadmap for Semiconductors).

Consensus roadmaps continue to project that the rate of change will settle to a more moderate 10% shrink per year to allow more time to develop new lithography

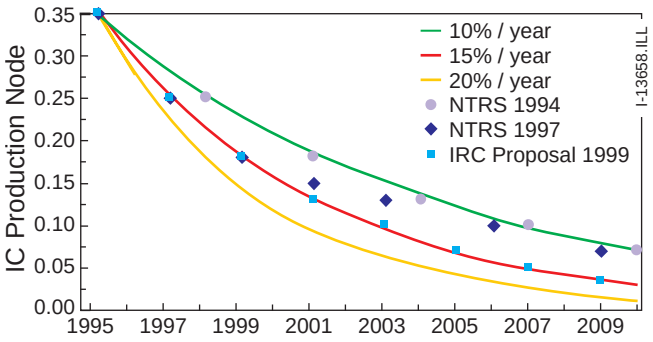

Figure 1 Lithography Roadmap for Semiconductors

technologies. However, these projections have so far underestimated the competitive drive of the IC industry and the innovation of lithographers. This evolution has been achieved through the transition from i-line to KrF lithography; the continuing innovations that have enabled the production of optical systems with

increasingly higher NA lenses; and the implementation of resolution enhancement techniques in production (Figure 2).

The industry originally projected the implementation of ArF lithography at the 180 nm node. However, this became superfluous with the advances in KrF lithography and the early introduction of the 180 nm node. The current production at 180 nm is achieved using KrF Step & Scan systems with an NA ≥ 0.6 together with annular illumination and limited application of attenuated Phase Shift Masks. The decision on preferred wavelength for production at the 130 nm node has yet to be finalized. It looks increasingly like KrF lithography, with the use of more resolution enhancement techniques, will be the preferred choice.

2. INTRODUCTION

This paper reviews the current capabilities of resolution enhancement techniques together with an advanced, 0.70 NA KrF Step & Scan system. This system features AERIAL II™, a new illuminator system, that enables fully-automated, continuous-variable, high-efficiency off-axis illumination (annular and QUAdrupole Shaped AnnulaR, QUASAR™), to address the 130 nm node. In this paper we focus on imaging enhancements created by the use of the off-axis illumination together with Binary Intensity Masks. The same illumination technique was used for dense lines/spaces as well as for isolated lines, bordered with scattering bars. First we analyzed imaging performance of both dense and isolated lines from a theoretical standpoint, using two simple models to examine the impact of illumination setting on both depth of focus and exposure latitude. The theoretical predictions were then compared with experimental results for 130 nm lines.

Finally, experimental results were used to draw conclusions about the viability of KrF lithography with the above enhancement techniques for mass production at the 130 nm node.

3. THEORETICAL

For dense lines with a half-pitch close to the resolution limit, off-axis illumination offers the unique possibility to optimize depth of focus and exposure latitude by adjusting the partial coherence settings (Figure 3). As explained in the next section, optimum settings for

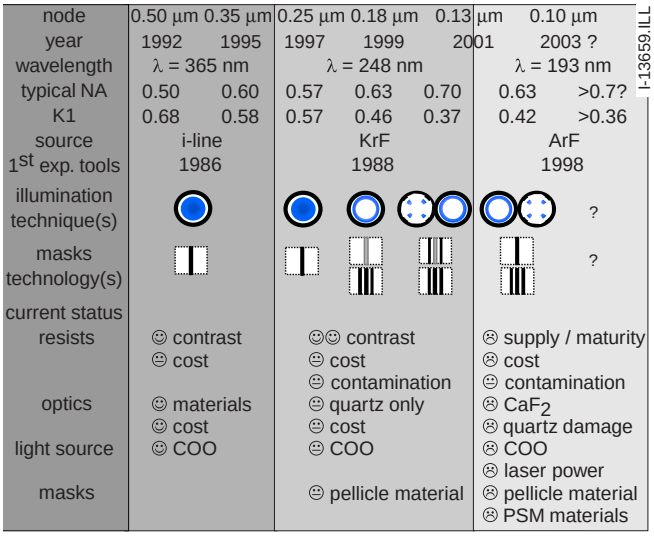

Figure 2 Comparison of Production Lithography Technologies

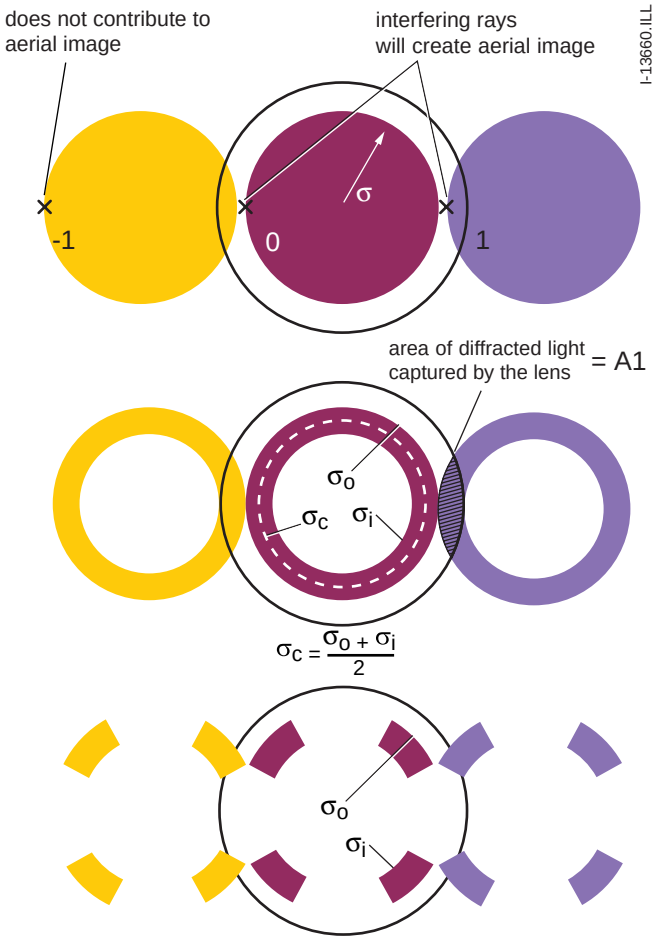

Figure 3 Definition of partial coherence in the case of conventional, annular and QUASAR™ illumination.

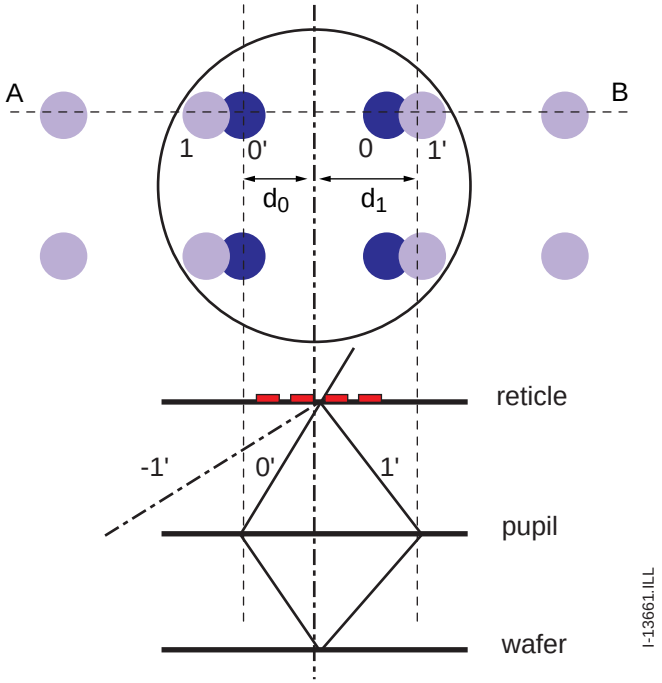

Figure 4 Schematic drawing of the pupil filling in the case of quadrupole illumination.

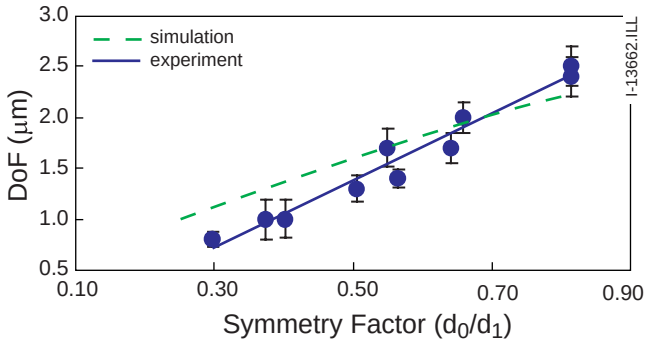

Figure 5 The circles indicate measured depth of focus vs. Symmetry Factor d_0/d_1 using QUASAR™ illumination. The Symmetry Factory d_0/d_1 was varied by changing the illumination setting.

- NA=0.6, 0.18 µm L/S, σ_o-$\sigma_i \approx 0.3$.

The dashed line indicates the same experiment, but depth of focus is simulated with Prolith™ using Lumped Parameter model, γ =18. NA=0.6, 0.18 µm L/S, σ_o-$\sigma_i \approx 0.3$.

depth of focus and exposure latitude can be different owing to the fact that both figures of merit are determined by two different physical phenomena. Both phenomena can be visualized by looking at the position of the diffracted orders in the entrance pupil of the projection lens (the pupil filling).

3.1 Analysis of the Depth of Focus for Fully-Dense Lines

Close to the resolution limit, the aerial image is formed by two-beam interference of the zero order and first order diffracted light. This is true, irrespective of illumination mode, whether conventional, annular or quadrupole, except with the application of Alternating Phase Shift Masks. This is shown schematically in Figures 3 and 4. The top part of Figure 4 shows the pupil filling when using quadrupole illumination. The cross-section AB is shown in the lower part of Figure 4. The more symmetrical the zero and first order rays are with respect to the main axis of the projection lens, the larger the depth of focus [2,3].

For optimum depth of focus, the illumination settings should be chosen such that the distance between the zero order and the projection lens axis (d_0) and the distance between first order and projection axis (d_1) are equal. This is accomplished by adjusting the radial placement of the illumination pole, i.e. the sigma center. An experimental verification of this behavior is shown in Figure 5 for 0.18 µm L/S, which were printed on an ASML PAS 5500/550 scanner using QUASAR™ illumination at an NA setting of 0.60.

The coherence settings, σ_o and σ_i, were modified so that the sigma center, $((\sigma_o + \sigma_i)/2)$ varied through the radius of the pupil while keeping the pole size (σ_o-σ_i) constant. The ratio of d_0 to d_1 was calculated for each illumination setting. Figure 5 shows the obtained depth of focus versus the Symmetry Factor d_0/d_1. As expected, highest depth of focus is obtained for Symmetry Factors close to one. Simulations using Prolith™ indicate the same trend.

Symmetry Factors close to one mean that the first order diffraction mode will overlap with the zero order coming from another pole as illustrated in Figure 4. In fact, using optimum illumination settings (d_0=d_1), the first order from one pole and 0 order from another pole will exactly overlap (pole 0 and 1' in Figure 4). It should be stressed that, although these poles will overlap (e.g. 0 and 1'), they will not interfere since there is no phase correlation between the four incident poles (e.g. 0 and 0'). In this way the overlap of the poles in the pupil-filling diagram can be used to identify

optimum illumination setting with respect to depth of focus. This visualization can also be used for other illumination settings, such as annular illumination. Using the constraint $d_1=d_0$ and simple diffraction theory, an analytic expression for the optimum pole position can be derived for quadrupole illumination [2,3] as follows:

$$\sigma_{center} = \frac{1}{LW}\left[\frac{\lambda}{NA}\right]\frac{\sqrt{2}}{4} \quad (1)$$

$$\sigma_{center} = \frac{\sigma_{outer} + \sigma_{inner}}{2} \quad (2)$$

3.2 Exposure Latitude for Dense Lines

Exposure latitude for dense lines depends significantly on the coherence settings and Numerical Aperture. To optimize exposure latitude the aerial image contrast has to be maximized [4]. The aerial image contrast depends on the amount of first order diffracted light that is captured by the projection lens. Figure 6 shows the experimentally-observed exposure latitude at a fixed annular illumination setting (PAS 5500/700, NA=0.7, σ_0=0.85, σ_i=0.55) for fully-dense lines with varying pitch.

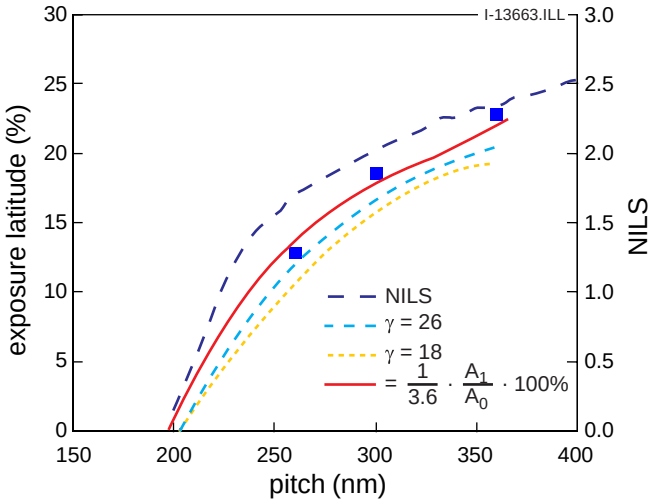

Figure 6 Figure 6: Squares indicate experimentally observed exposure latitude of fully-dense lines (L/S=1:1) for varied pitches.

- annular illumination (NA=0.7, σ_0=0.85, σ_i=0.55) Solid line indicates exposure latitude calculated from pupil filling diagram. Dashed lines:
- exposure latitude calculated by PROLITH™, using a lumped parameter model and γ=18 and 26.
- Normalized Image Log Slope (NILS) calculated by PROLITH™

Decreasing the feature pitch will lead to a reduced amount of first order light being captured by the lens, and thus to a decreased exposure latitude. Again the pupil filling can be used to depict this schematically. In the same figure, the exposure latitude has been derived from the pupil filling diagram as follows:

$$Exp.\ lat. = \frac{1}{C} \bullet \frac{A_1}{A_0} \bullet 100\% \quad (3)$$

Where:

A_1 = the amount of first order light captured by the lens

A_0 = the total amount of zero order light

Both values can be determined by computing the respective areas in the pupil-filling diagram. The correlation factor C takes into account the behavior of different resists (resist contrast) and was 3.6 in this example. Therefore, this method can be used to determine the relative contrast of one resist compared to another. As can be seen, the pupil-filling analysis indicates the same trend as the experimental results. The exposure latitude was also determined using

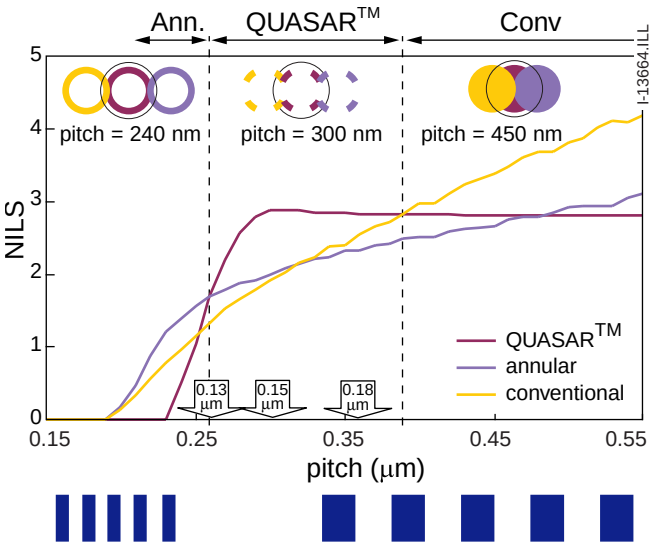

Figure 7 Simulated normalized image logslope for fully-dense structures (L:S = 1:1) of various pitches

conventional: NA=0.7 σ=0.85

annular: NA=0.7, σ_0=0.85, σ_i=0.55

QUASAR™: NA=0.7, σ_0=0.85, σ_i=0.55

Prolith™ (Lumped Parameter Model, resist contrast γ=16 and 26). Prolith™ simulations agree very well with experimental results and pupil-filling analysis.

Using the simulator, and avoiding the implementation of resist parameters, the normalized image log-slope NILS is another good measure to compare and optimize aerial image contrast and exposure latitude. The NILS was calculated for fully-dense lines (L:S=1:1) and different feature sizes using annular, QUASAR™ and conventional illumination at an NA of 0.7 with the highest possible coherence settings. Results are shown in Figure 7.

For very large features, conventional illumination provides the highest aerial image contrast. For feature size approaching the resolution limit, QUASAR™ is the preferred illumination setting whereas annular illumination provides the best aerial image contrast at the resolution limit. Thus, to image fully-dense lines with pitches in the range 260 nm to 460 nm, QUASAR™ is the preferred illumination setting on the PAS 5500/700 system. As conventional illumination does not provide sufficient exposure latitude at the feature sizes being investigated, we will not consider this illumination mode in the rest of the paper.

Besides depth of focus and exposure latitude, another critical factor in extending KrF lithography to 130 nm features is the Mask Error Factor (MEF). It has been shown that the higher the aerial-image contrast, the lower the Mask Error Factor [4]. For binary masks and fully-dense 130 nm lines the MEF is significantly larger than 1. Therefore reticle errors will cause large contributions to the CD uniformity budget. Extending KrF lithography to the 130 nm regime requires optimization of image contrast to enhance EL and decrease MEF.

3.3 Depth of Focus and Exposure Latitude for 130 nm Lines with Different Pitches

In this paper, we will study the impact of illumination settings on process window (depth of focus and exposure latitude) for 130 nm lines with pitches in the range from 260 nm (fully-dense) to fully-isolated. Figure 8 shows the simulated depth of focus for 130 nm lines of different pitch. Simulations were done using Prolith™ version 6.05 and applying a lumped parameter model (resist contrast γ=18). Again annular and QUASAR™ illumination were compared at a fixed illumination setting of NA=0.7, σ_o=0.85, σ_i=0.55.

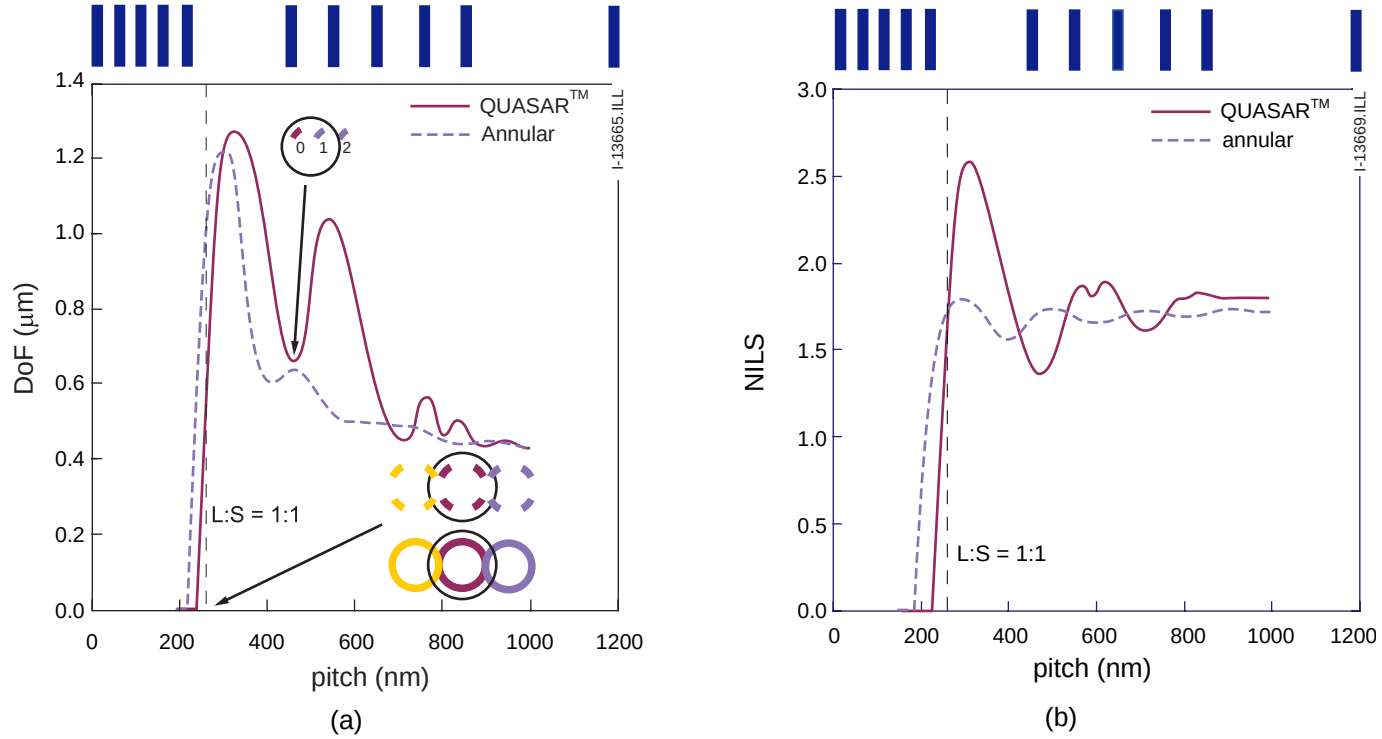

Figure 8 Figure 8: (a) simulated depth of focus vs. pitch for 130 nm lines using QUASAR™ and annular illumination. NA=0.7, σ_o=0.85, σ_i=0.55
(b) simulated aerial image contrast (NILS) vs. pitch for 130 nm lines using QUASAR™ and annular illumination.

For fully-dense lines (L:S=1:1) annular illumination will give slightly higher depth of focus. This trend can be easily explained when looking at the pupil filling (Figure 8). For annular illumination, the diffracted orders are more symmetrical with respect to the optical axis (larger overlap of the zero and first order). For dense lines with pitches larger than 0.26 µm, QUASAR™ will give superior depth of focus. For fully-dense lines, the exposure latitude is the same for annular and QUASAR™. Again this can be predicted by the exposure latitude from the pupil filling using equation 3. For slightly relaxed pitches QUASAR™ will give significantly more aerial-image contrast.

A significant change in both the depth of focus versus pitch and NILS versus pitch, can be observed around a pitch of 480 nm in the case of QUASAR™ illumination. This is related to the contribution of second-order diffracted light in the aerial image, as shown in the pupil-filling diagram in Figure 8.

For the more isolated lines the depth of focus will gradually decrease for all illumination modes when using Binary Intensity Masks. This is one of the main limitations in low-k1 lithography. To overcome this, scattering bars can be applied to make the diffraction pattern of isolated lines appear similar to that of dense

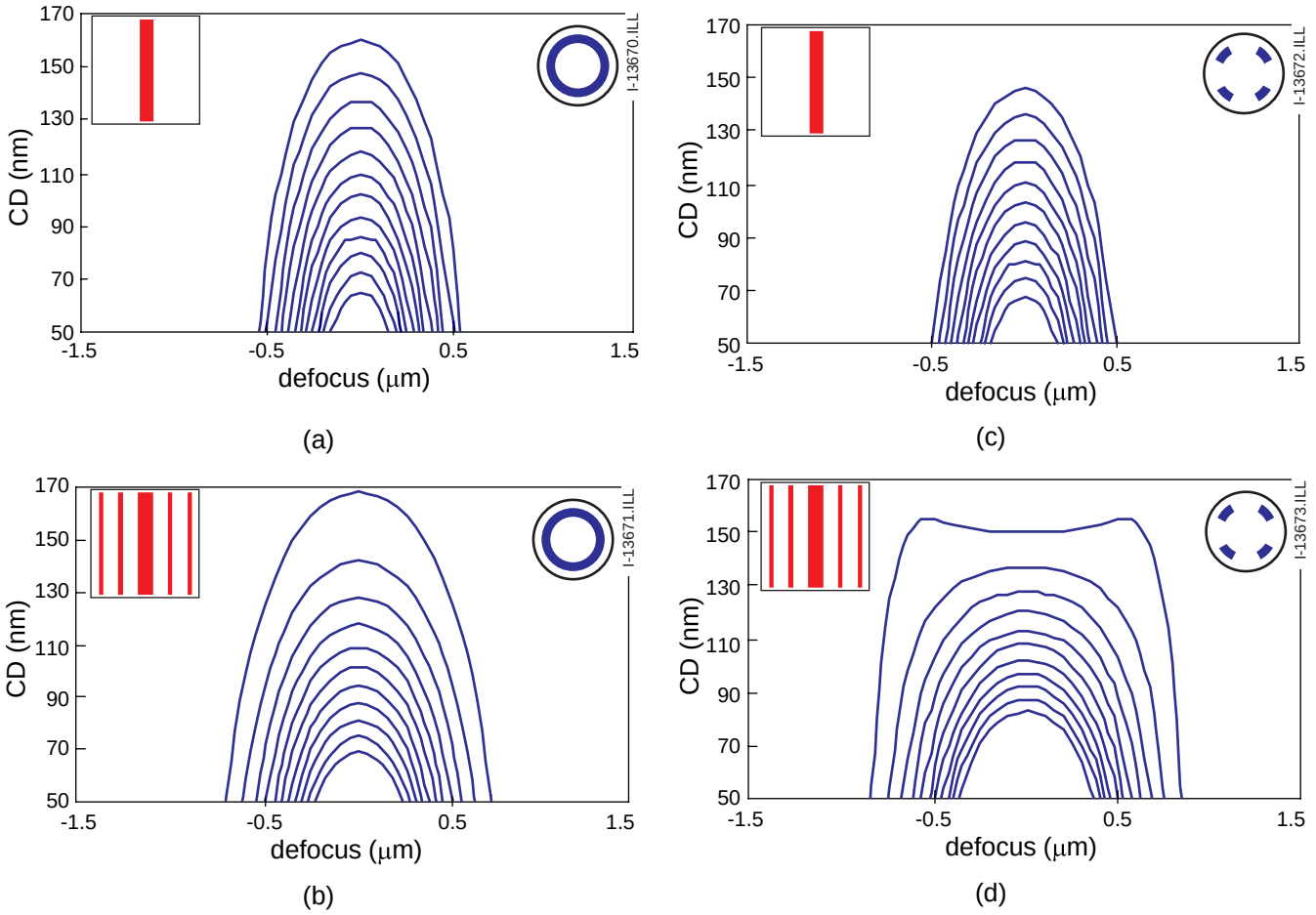

Figure 9 Bossung curves for annular and Quasar™ illumination, NA=0.7, σ_o=0.85, σ_i=0.55, 130 nm isolated lines, simulations using PROLITH™ 6.05

a) no assisting features, annular
b) assisting features, annular
c) no assisting features, QUASAR
d) assisting features, QUASAR

Size of scattering bars: 60 nm, pitch of scattering bars 300 nm. Energy steps are 0.05* Energy to size

lines [5]. Applying scattering bars has a big impact on the depth of focus. This is schematically shown in Figure 9. For isolated lines without scattering bars, the depth of focus is limited. This is illustrated by the strong curvature in the Bossung graph; the iso-focal CD for isolated lines differs significantly from the nominal CD. The application of QUASAR™ and annular illumination gives similar results (Figure 9 a and c). Depth of focus can be enhanced applying two scattering bars on each side of the isolated line. The strongest enhancement is achieved when scattering bars are applied in combination with QUASAR™ illumination (Figure 9d). For this setting the iso-focal CD is close to the nominal CD, resulting in a considerable improvement in the depth of focus.

Applying scattering bars also reduces proximity effects. Optical proximity effects are due to the fact that the diffraction patterns for dense and isolated lines are very different. The use of scattering bars will decrease this difference resulting in a reduced iso-to-dense bias.

4. EXPERIMENTAL CONDITIONS

Exposures were performed using QUASAR™ and annular illumination modes on an ASML PAS 5500/700 high NA scanner. QUASAR™ is ASML's proprietary quadrupole illumination mode, which utilizes diffractive optical elements in combination with the zoom optics of the AERIAL™ illuminator. The use of optics to generate the QUASAR™ pupil filling enables high illumination intensity to be maintained hence minimal

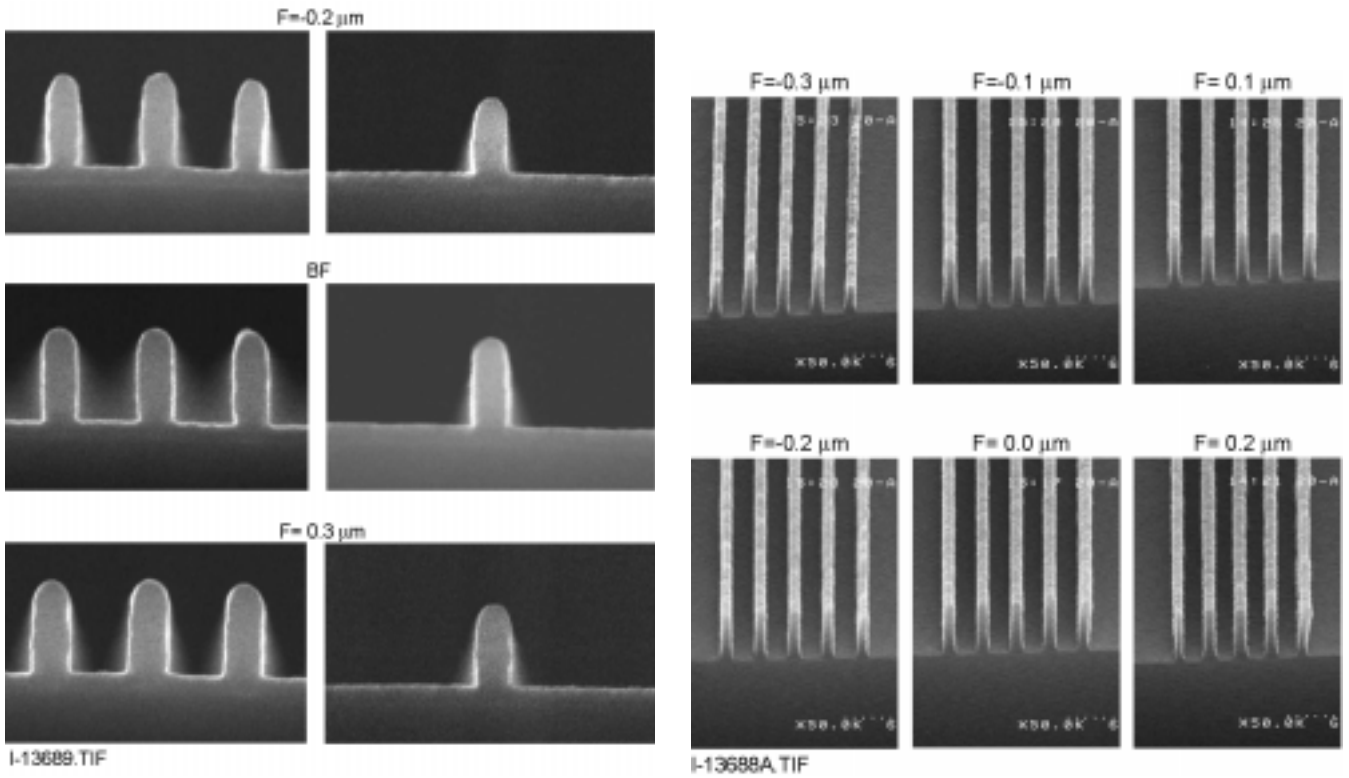

Figure 10 Figure 10: cross-section SEM pictures for different 130 nm features using the optimum illumination mode for every feature type. NA= 0.7, σ_o=0.85, σ_i=0.55. 400 nm Shinetsu 463 DUV resist
(a): semi-dense lines (L/S=1:1.5), substrate AR2, QUASAR™
(b): fully-isolated features using assisting features, substrate AR2, QUASAR™
(c): fully-dense features (L/S=1:1), substrate SiON, ANNULAR

loss of wafer throughput. An additional feature of annular and QUASAR™ illumination on the PAS 5500/700 is that the partial coherence parameters σ_o and σ_i can be adjusted over a wide range of settings using fully-integrated software control.

Shinetsu SEPR-463 DUV resist was used at a thickness of 400 nm. A 60 nm BARC (Shipley AR2) was applied to reduce reflections from the substrate. Top down CD measurements were performed using either a Hitachi 8C40 or an AMAT OPAL 7830 SI top-down SEM. Figure 10 shows SEM cross-sections for fully-dense (L:S=1:1), semi-dense (L:S=1:1.5) and isolated features. The photographs were taken over the typical focus range for our CD uniformity tests (0.4-0.6 μm).

5. RESULTS

In this section the predicted impact of off-axis enhancement techniques, such as annular and QUASAR™, are experimentally verified. The final goal is to show sufficient focus-exposure process latitudes and CD uniformity for dense and isolated lines.

5.1 Process Latitude of Fully-Dense, Semi-dense and Isolated Lines

130 nm dense lines were exposed with annular and QUASAR™ illumination (NA=0.7, σ_0=0.85, σ_i=0.55). The experimental Bossung curves can be seen in Figure 11a and b. It was noticed that, due to limited adhesion between the BARC and photo-resist, resist

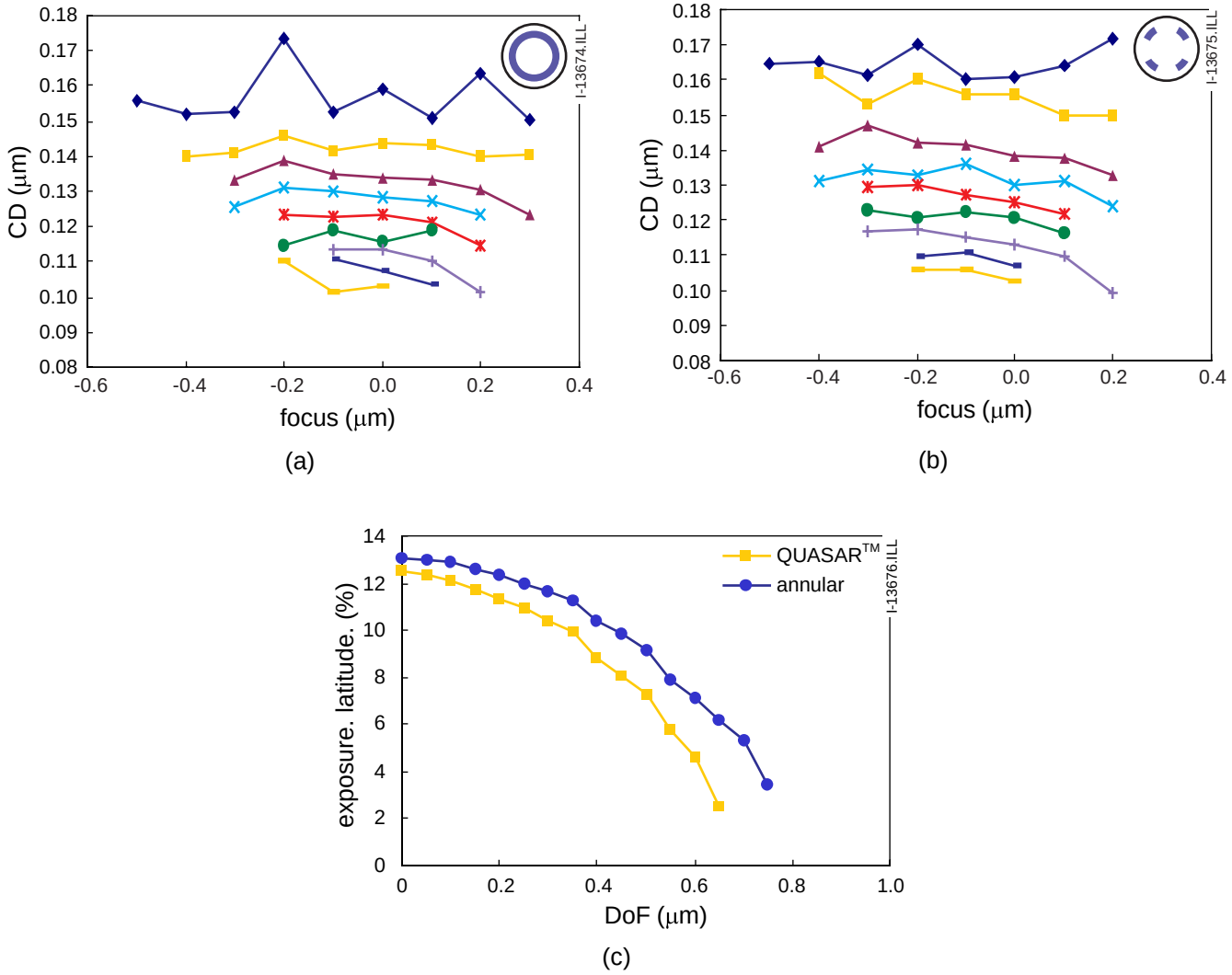

Figure 11 (a) & (b): measured Bossung curves for fully-dense lines using annular and QUASAR™ illumination. NA=0.7 σ_0=0.85, σ_i=0.55. Energy steps are 1 mJ, dose to size ≈ 30 mJ
(c): experimentally observed process latitude, derived from the Bossung curves in figure 11a & b.

lines lifted off in over-exposed and negative defocus conditions. Use of an inorganic BARC (SiON) was found to reduce this problem considerably.

The Energy-Defocus (ED) windows were determined from the Bossung curves using PRODATA™ (by FINLE). By fitting rectangular boxes to the ED-windows, the process latitudes could be derived. These process latitudes were used as a figure of merit to compare the different illumination modes. The experimental process latitudes are plotted in Figure 11c and confirm the expectation from the pupil diagrams as outlined in the theoretical section.

Based on these results the annular illumination setting provides a reasonable process latitude for 130 nm fully-dense lines (0.55 μm depth of focus at 8% exposure latitude). This is also supported by the CD uniformity results discussed in the next chapter (see Figure 16). For semi-dense 130 nm features (L:S=1:1.5, pitch = 325 nm) QUASAR™ provides larger process latitudes. The experimentally determined DoF was 0.9 μm for QUASAR™ illumination and 0.7 μm for annular illumination (NA=0.7, σ_o=0.85, σ_i=0.55). In addition to the DoF improvements, and as expected from the theoretical predictions, exposures using QUASAR™ were found to yield much higher exposure latitude, i.e., 22% compared to 12% for annular.

For isolated lines the depth of focus is clearly the performance-limiting factor. In Figure 12, the measured Bossung curves for fully-isolated lines are graphed for QUASAR™ illumination. Applying two assisting lines at each side of the main feature, the Bossung curves can be flattened considerably.

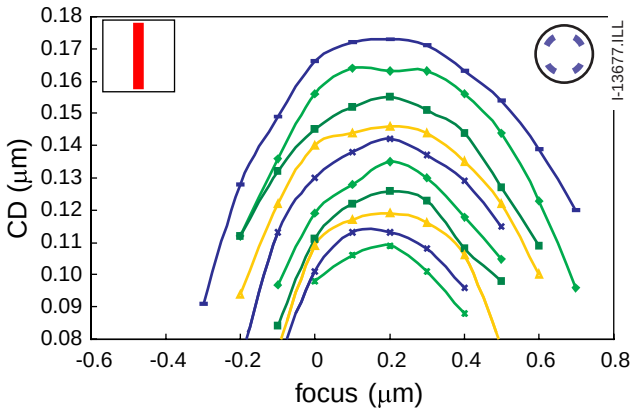

(a)

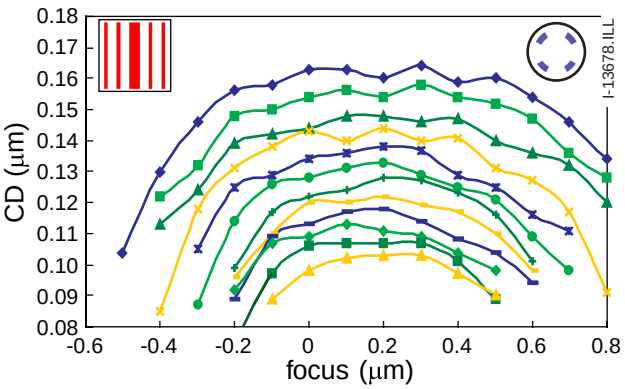

(b)

Figure 12a measured Bossung curves for fully-isolated 130 nm lines using QUASAR™ illumination. NA=0.7 σ_o=0.85, σ_i=0.55. Energy steps are 1 mJ.

Figure 12b measured Bossung curves for 130 nm isolated lines and scattering bars using QUASAR™ illumination. NA=0.7 σ_o=0.85, σ_i=0.55. Scattering bar width=80 nm. Scattering bar pitch = 260 nm.

Figure 13 shows top-down CD-SEM photographs for both cases. By applying assist bars, an 80% increase in focus latitude was achieved. For 100 nm isolated features, a similar DoF gain was observed when using assist bars of 60 nm. From the top-down CD-SEM measurement, the DoF was determined to be 0.4 µm without assisting features, and 0.75 µm with assisting features.

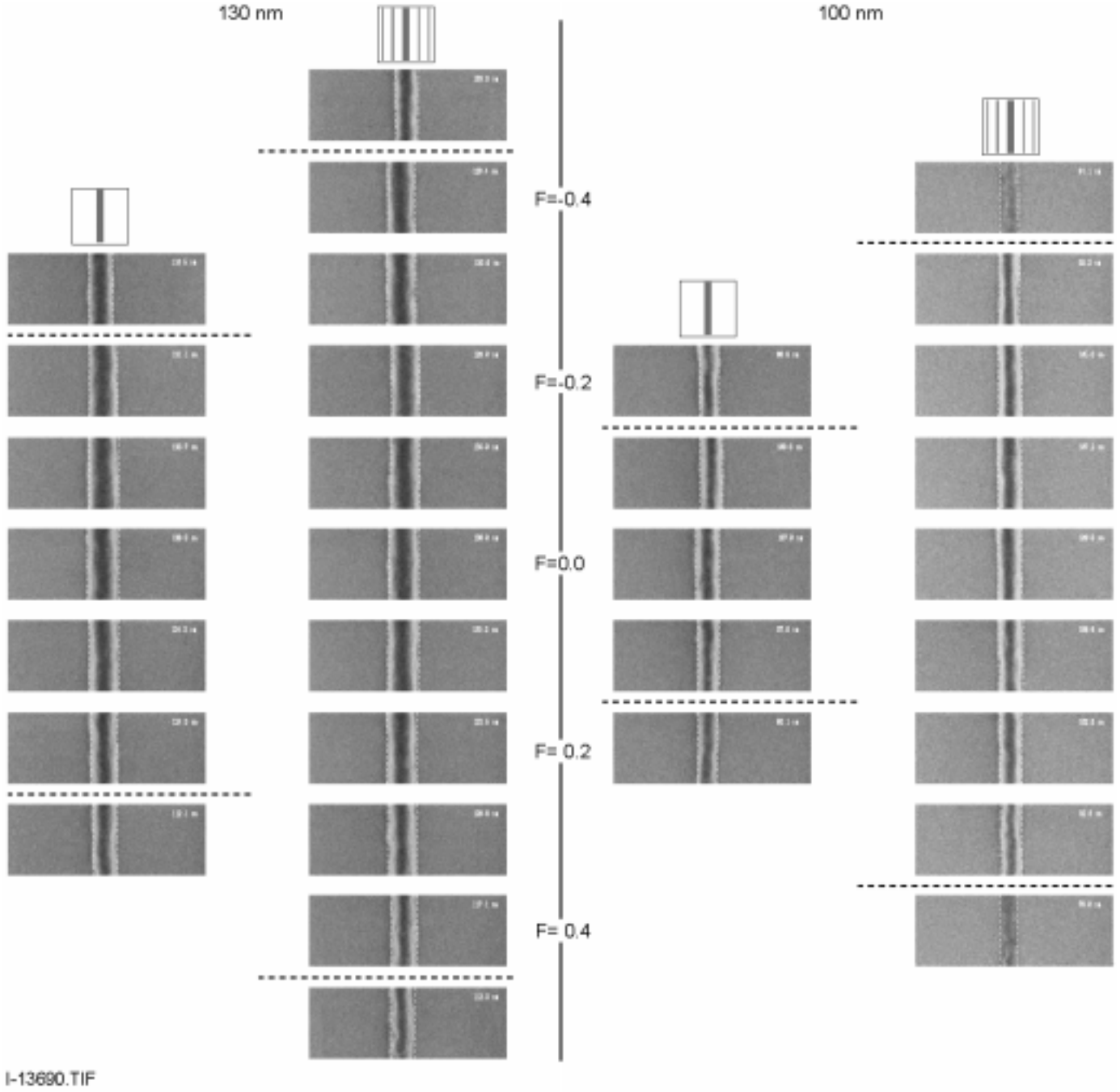

Figure 13 Top-down SEM pictures for 130 nm and 100 nm isolated lines using QUASAR™ illumination. Left side: without assisting features. Right side: with two assisting features at each side (80 nm width for 130 nm, 60 nm for 100 nm features

The depth of focus gain is a function of the width and placement of the assisting features. A design of experiment was performed for the 130 nm isolated lines, varying the size and placement of the scattering bars. The outcome of this experiment is graphed in Figure 14. The best results were obtained for an assist width of 80 nm and an assist pitch of 260 nm. The printing of assist features was not observed within the Energy-Defocus range for ±10% CD variation. In Figure 15 process latitudes for optimized assist width and placement, using annular and QUASAR™ illumination modes, are compared to the case with no assisting features. In addition to the improvement in depth of focus, a 25% increase in exposure latitude was also observed.

Table 1 summarizes experimental process latitude for 130 nm features. For fully-dense lines, annular illumination will give the best process window. For semi-dense to isolated pitches (and looking at horizontal and vertical structures), QUASAR™ will be the preferred illumination setting. For isolated lines, optimum performance is achieved when assisting features are combined with QUASAR™ illumination mode. In this case the process window is larger than that observed for fully-dense L/S.

Table 1 Process latitudes (max. depth of focus in µm and max. exposure latitude in %) for fully dense, semi-dense and fully-isolated 130 nm features. NA=0.7, σ_o=0.85, σ_i=0.55. The shading indicates the preferred illumination mode for the different features.

130 nm features	L:S=1:1		L:S=1:1.5		fully isolated, no scattering bars		fully isolated with scattering bars	
	DoF	EL	DoF	EL	DoF	EL	DoF	EL
QUASAR™	0.65	12.5	0.9	22	0.5	16	0.95	18
Annular	0.9	13	0.7	12	0.5	13	0.75	16

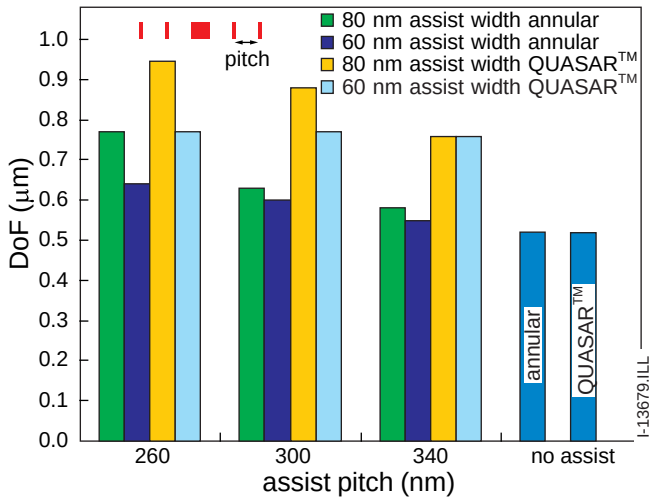

Figure 14 The impact of assist-feature width and placement on the experimentally observed depth of focus for 130 nm isolated lines using QUASAR™ and annular illumination (NA=0.7, σ_o=0.85, σ_i=0.55)

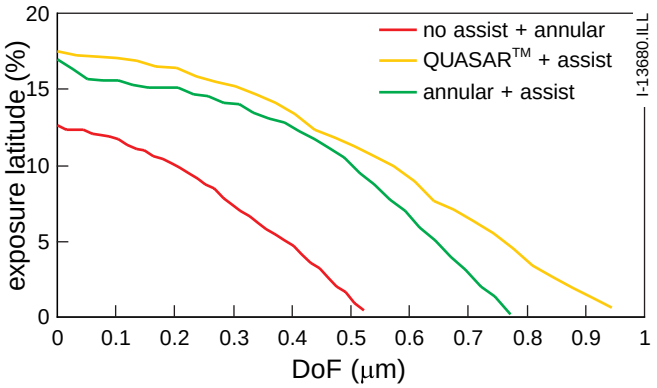

Figure 15 Experimentally determined exposure latitude vs. depth of focus:

- annular and fully-isolated 130 nm lines
- annular and assisting features, 80 nm width, 260 nm pitch, 130 nm isolated line
- QUASAR™ and assisting features, 80 nm width, 260 nm pitch, 130 nm isolated line

NA=0.7 σ_o=0.85, σ_i=0.55

6. CD UNIFORMITY AND MASK ERROR FACTOR

Comparing the results for dense lines and semi-dense with optimized assist features it is clear that fully-dense lines are likely to be more critical for CD control, due to their smaller process window. The smaller exposure latitude of 130 nm dense lines will make the Mask Error Factor (MEF) a more critical factor for CD uniformity. Exposure latitude for fully-dense lines was found to be about the same for both annular and QUASAR™ illumination.

The CD uniformity of 130 nm dense lines as a function of focus for annular illumination can be seen in Figure 16a. The CD uniformity within the exposure field was determined by measuring both horizontal and vertical features at 20 positions. The CD uniformity (range) across the scanner exposure field at best focus is 21 nm. By averaging over 6 identically exposed dies, the process-related and CD metrology-related noise could be reduced. CD uniformity was 16 nm at best focus after averaging. The CD uniformity deteriorated away from best focus due to the larger MEF as supported by the plot of MEF versus defocus in Figure 16b. At best focus, the MEF was found to be 2.6 while, out of focus, it rapidly increased to values greater than 3. Even without subtracting reticle CD contribution, a CD control of better than ± 10% (26 nm range) across a 0.6 μm focus range was achieved. By using the same coherence settings for QUASAR™ illumination similar results were obtained. CD uniformity was 15 nm at best focus after averaging over 6 dies. The range of Mask CD variations on the picked CD reticle [6], used for the CD uniformity test, was 18 nm (@4x).

It is expected that further improvement of CD control can be achieved by either improving reticle CD control or by using (alternating or attenuated) Phase Shift Masks. These masks generate higher aerial image contrast and thus improve the MEF. By using alternating Phase Shift Masks, an MEF of 1.4 was observed at best focus for 125 nm L/S (L:S = 1:1) under similar conditions (exposure tool and resist process) [7].

As isolated lines with assisting features and QUASAR™ illumination have been shown to exhibit larger process latitudes than dense lines, better CD control is expected. The CD uniformity through focus for isolated 130 nm lines using QUASAR illumination (NA=0.7 σ_o=0.85, σ_i=0.55) can be seen in Figure 17. CD uniformity was determined across the scanner slit for 5 positions (horizontal and vertical features). Two

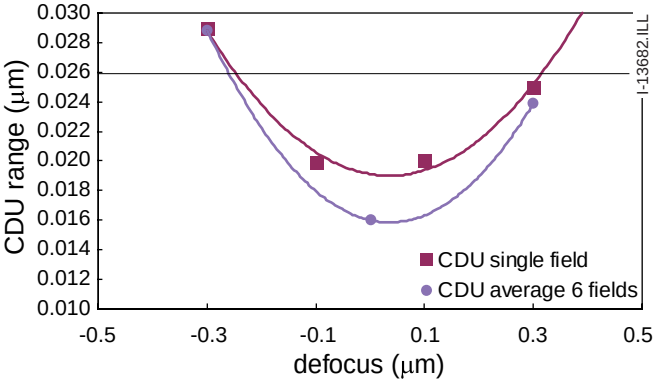

(a)

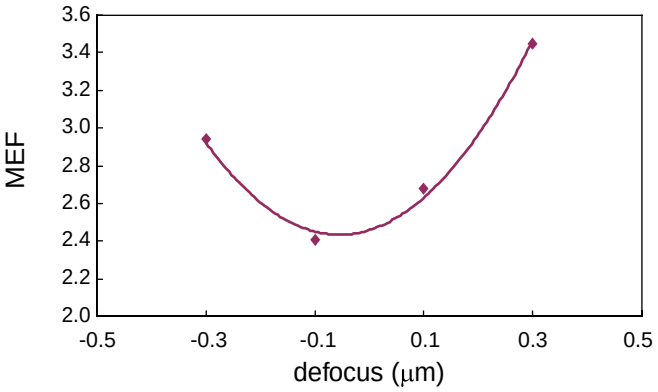

(b)

Figure 16a measured CD-uniformity (range, μm) at different defocus levels for annular illumination. NA=0.7 σ_o=0.85, σ_i=0.55 130 nm L/S (L:S = 1:1)

Figure 16b measured Mask Error Factor vs. defocus for the same illumination setting

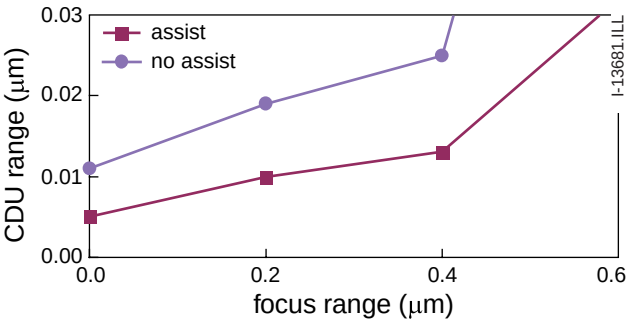

Figure 17 CD uniformity through focus across the scanner slit (5 positions in the slit, horizontal and vertical features) for QUASAR™ illumination.
- 130 nm isolated line
- NA=0.7 σ_o=0.85, σ_i=0.55
- Assist width = 80 nm, assist pitch= 260 nm

cases were compared: isolated lines without assist features and isolated lines with two assist features at each side. Applying assist features clearly improves the CD Uniformity. At best focus, this improvement is partly due to the improved exposure latitude. Through focus, the enhanced DoF clearly helps to decrease the CD uniformity in the case of assist features. Using optimized assist width and placement, CD uniformity of 5 nm at best focus, and 13 nm over a 0.4 μm focus range was achieved. The measured reticle CD variations were 18 nm (@4x).

7. CONCLUSION AND OUTLOOK

Our results indicate that KrF Step & Scan lithography with an NA of 0.7, combined with off-axis illumination and reticle enhancements, is a viable candidate for production at 130 nm feature sizes.

Annular illumination is the optimum off-axis illumination mode for 130 nm dense lines (L:S=1:1). Under annular illumination conditions (NA=0.7, σ_o=0.85, σ_i=0.55) an exposure latitude of 13% and a depth of focus of 0.8 μm was achieved for 130 nm dense lines. Under the same conditions, we obtained a CD uniformity of 16 nm range at best focus, and 26 nm over a 0.6 μm focus range.

QUASAR™ has been determined to be the optimum illumination mode for isolated to semi-dense lines (L:S=1:1.5). Using QUASAR™ illumination in combination with assisting features was shown to significantly increase both depth of focus and exposure latitude. Depth of focus could be increased from 0.5 μm to 0.95 μm by optimizing the width and placement of the assisting features. CD uniformity range across the slit was 5 nm at best focus and 13 nm over a 0.4 μm focus range.

In the future, the focus will be on the use of attenuated Phase Shift Masks for fully-dense features. Simulations using Prolith™ show an exposure latitude increase of 34% while going from a binary intensity mask to a 6% transmission attenuated Phase Shift Mask. Since the blanks for this mask technology in KrF lithography are becoming widely available, this is a cost-effective way to reduce the MEF, and thus improve the CD control for dense lines. For semi-dense to isolated pitches, the assisting feature route looks very promising. DoF values close to 1 μm are reported in this paper. A point of further investigation is the manufacturability and CD control of the assisting features on the mask. Recent experiments using a laser patterning tool showed assisting features down to 200 nm (@ 4x) with a very good linewidth control. Applying scattering bars also has a large impact on proximity effects. At the moment proximity effects are being characterized and the overlapping process window for a range of pitches is being calculated. Results will be reported elsewhere.

8. ACKNOWLEDGEMENTS

The authors would like to thank Jouke Krist, Ton Kiers, Gert-Jan Janssen for their support in exposing, measuring and analyzing the wafers and the Publications department (Vivian Kim and Frank Harmsen) for preparing this manuscript. Jacques Waelpoel is acknowledged for his help in designing the “assist feature mask.”

9. REFERENCES

[1] Gordon E. Moore et al., “Lithography and the future of Moore's law”, SPIE Vol. 2440 1995.
[2] J. Finders et al.,” Sub-0.25 micron lithography applying quadrupole illumination on a DUV step-and-Repeat system”, Proceedings Olin Lithography Conference “Interface”, 1998.
[3] D. Nam et. al, “Lithography of 180 nm design rule for 1-Gb DRAM” SPIE Vol. 3334, 1998.
[4] J. van Schoot et al., “Mask error factor: causes and implications for process latitude”, SPIE Vol. 3679,1999.
[5] J.F. Chen et al., “Practical method for full-chip optical proximity correction”, SPIE Vol. 3051, 1997.
[6] J. Waelpoel et. al, “Demonstrating next-generation CD uniformity with today's tools and processes”, SPIE Vol. 3236, 1998.
[7] Koen van Ingen Schenau et al., “Towards a production worthy 0.13 μm process using alternating phase shift masks”, Proceedings Arch Lithography Conference “Interface” 1999.